IOP Conf. Series: Materials Science and Engineering **188** (2017) 012004 doi:10.1088/1757-899X/188/1/012004

Biosynthesis and characterization of ZnO nanoparticles using the aqueous leaf extract of *Imperata cylindrica L.*

I S Saputra and Y Yulizar

Department of Chemistry, Faculty of Mathematics and Natural Sciences Universitas Indonesia, Kampus UI Depok, Depok 16424, Indonesia

Corresponding author's e-mail: yokiy@ui.ac.id

Abstract. ZnO nanoparticles (ZnO NPs) were biosynthesized.The growth was observed by a sol-gel method. ZnO were successfully formed through the reaction of zinc nitrate tetrahydrate $Zn(NO_3)_2.4H_2O$ precursor with aqueous leaf extract of *Imperata cylindrica L* (ICL). The structural and optical properties of ZnO were investigated. The as-synthesized products were characterized by UV-Visible (UV-Vis), UV diffuse reflectance spectroscopy (UV-DRS), Fourier transform infrared spectroscopy (FTIR), X-ray diffraction (XRD), scanning electron microscopy (SEM), and energy-dispersive X-ray spectroscopy (EDS). UV-Vis absorption data showed hydrolysis and characteristic of absorption peak at 300 nm of $Zn(OH)_2$. UV-DRS confirmed that ZnO NPs has the indirect band gap at 3.13 eV. FTIR spectrum revealed the functional groups and indicated the presence of protein as the capping and stabilizing agent on the ZnO surface. Powder XRD studies indicated the formation of pure wurtzite hexagonal structure with particle size of 11.9 nm. The detailed morphological and structural characterizations revealed that the synthesized products were hexagonal nanochip.

Keywords: ZnO nanoparticles, *Imperata cylindrica L.*, biosynthesis, sol-gel method and stabilizing agent.

1. Introduction

In recent years, metal nanoparticles are important concern for researchers [1]. Zinc oxide is an inorganic compound appears as white powder, and insoluble in water. The powder is widely used as an additive for numerous materials and products, including plastics, ceramics, glass, cement, batteries, etc. ZnO is found in the earth crust as zincite mineral. In materials science, ZnO is called II-VI semiconductor [2]. ZnO is a semiconductor and piezoelectric material with a direct wide band gap of 3.37 eV and a large exciton binding energy of 60 meV at room temperature [3].

There are several methods reported for the synthesis of ZnO nanoparticles (ZnO NPs), which include chemical vapor deposition, gas-phase method, spray pyrolysis, hydrothermal synthesis, micro emulsion, electrochemical method, pulsed laser deposition, microwave synthesis, and the sol-gel method [4]. The use of environmentally benign materials such as plant extract, fungi, and bacteria for generating metal or metal oxide NPs is considered as an eco-friendly approach [5-8]. ZnO is employed for a variety of important potential applications, such as antimicrobial activity [9], gas sensors [10], photocatalytic [11], and degradation of congo red organic dye [12].

The green synthesis of ZnO NPs using *Plectranthus amboinicus* leaf extract showed the morphology of rod shape with an average size of 88 nm [13]. The synthesis of ZnO NPs using *Aspalathus linearis* natural extract, as eco-friendly material, acted as reducing/oxidizing agent [14]. Characterization by

TEM image and XRD showed the ZnO NPs have an average diameter ranges from 1.0-8.5 nm. The crystal structures of ZnO exhibited a wurtzite, zinc blende, and rocksalt. *Agathosma betulina* natural extract was used in ZnO NPs formation as an effective chelating agent [15]. Based on the background in the present study, ZnO NPs formation is conducted using *Imperata cylindrica L.* leaf extract as a base source and stabilizing agent by sol-gel method.

2. Materials and methods

2.1. Preparation of the leaf extract

Imperata cylindrica L. (ICL) plant leaves were taken from Universitas Indonesia area. 5 g of dry powder ICL leaf was stirred with 100 mL of double distilled water for 1 h at 70°C until the colour of the colloid changes to light yellow. The extract was filtered with Whatman No. 1 paper filter.

2.2. Biosynthesis of ZnO NPs

25 ml of the extract was added with 3 g of $Zn(NO_3)_2.4H_2O$ under continuous stirring at 85°C for 24 h. This paste was heated in a furnace at 400°C for 4 h.

2.3. Characterization of ZnO NPs

The UV-Vis absorption spectrum was recorded using (Shimadzu UV-Vis 2600) spectrophotometer. UV-Vis diffuse reflectance spectra were observed by (UV-Vis DRS, Shimadzu 2450) in the wavelength range of 200-800 nm. The functional group of compound was examined using Fourier transform infrared spectroscopy (FTIR) (Shimadzu, Prestige 21). The crystal phase information was characterized from 20°-70° by XRD (Shimadzu 610) with Cu Kα (λ = 0.1546 nm) radiation. The surface morphology of ZnO NPs was examined by scanning electron microscope (SEM), and the chemical composition of the product was examined by energy dispersive X-ray spectroscopy (EDX, AMETEK).

3. Results and discussion

3.1. UV-Vis absorption and DRS spectroscopy analysis

Figure 1 shows the UV-Vis absorption spectra of ICL extract at maximum wavelength, λ_{max} 273 nm. The spectrum reveals a characteristic absorption peak of $Zn(OH)_2$ at λ_{max} of 300 nm wavelength. Hydrolysis of $Zn(NO_3)_2.4H_2O$ into $Zn(OH)_2$ produces a strong red shift. The DRS spectrum of ZnO NPs in figure 1b showed at the λ_{max} of 359 nm. The reflectance spectrum was analyzed using the Kubelka-Munk equations (equation 1):

$$F(R) = \frac{(1-R)^2}{2R} \quad (1)$$

where *R* is the reflectance value, F (*R*) is the equivalent to the absorption coefficient. The band gap energy (Eg) of ZnO NPs was estimated from the variation of Kubelka-Munk function with photon energy [16]. Figure 2 shows the Kubelka-Munk plots of ZnO NPs that used to determine association of Eg with its indirect transitions. The ZnO NPs exhibits the indirect Eg of 3.13 eV.

3.2. FT-IR spectroscopy

The FT-IR spectrum of ZnO NPs (figure 3) shows the wavenumbers at 3375, 2349, 1375, 915 and 481 cm^{-1}, respectively. The broad peak at 3375 cm^{-1} indicated the -OH stretching vibrations. The peak at 2349 cm^{-1} indicated the free –C=O group. Stretching vibrations present at 1375 cm^{-1} showed C-O-H bending mode. The peak at 915 cm^{-1} showed the characteristic -NH of amine. The band at 481 cm^{-1} confirmed the stretching vibrations of ZnO NPs. The ICL leaf extract containing polyols, terpenoids, and proteins that has functional groups of amines, alcohols, ketones, and carboxylic acid contributed in hydrolysis and acted as stabilizing agent. The good stability of ZnO NPs is due to the free amino and

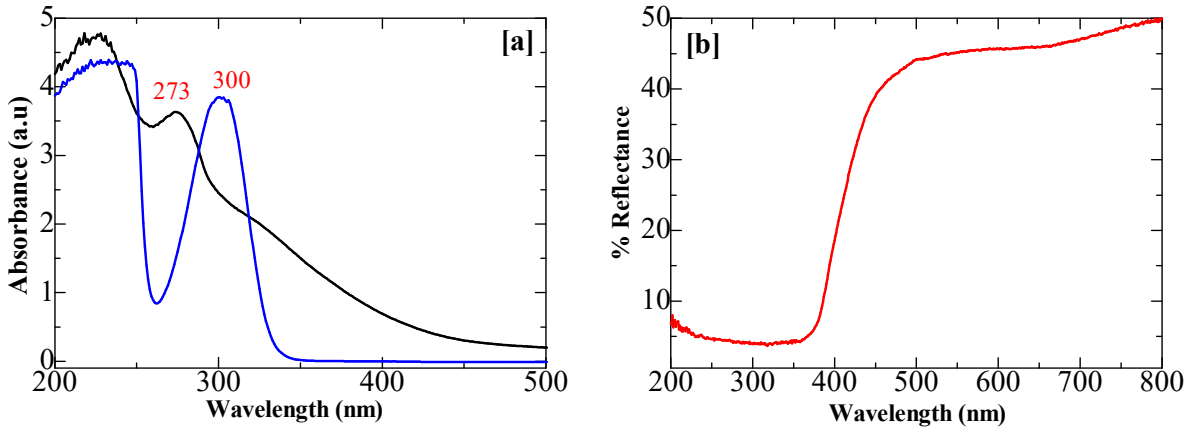

(a) (b)

Figure 1. (a) UV-Vis absorption and (b) DRS spectrum of biosynthesized ZnO NPs.

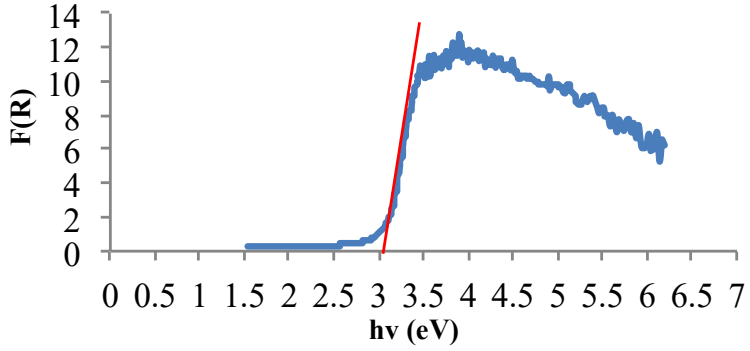

Figure 2. Plot of indirect band gap energy of ZnO NPs.

carboxylic groups interacted with the ZnO NPs surface. The bonds of functional groups such as –C-O-C-, C-O- and -C=C- were derived from heterocyclic compounds, and the amide bonds derived from the proteins in ICL leaf extract, and acted as capping agent of ligands of the nanoparticles[17].

3.3. XRD analysis

The XRD patterns of the calcined ZnO NPs 800°C are shown in figure 3b. XRD pattern confirmed the crystal phase and crystallinity of ZnO NPs. The XRD peaks are adjusted with the JCPDS data card 89-1397 of ZnO hexagonal [18]. The detected peaks corresponded to the hexagonal phase ZnO NPs are found in the lattice planes (h,k,l) of (1 0 0), (0 0 2), (1 0 1), (1 0 2), (1 1 0), (1 0 3), (1 1 2), and (2 0 1) in the 2θ value : 31.71°; 34.37°; 36.18°; 47.49°; 56.57°; 62.85°; 68.01° and 68.98° respectively. The average grain size of sample was calculated using the Scherer's (equation 2).

$$D = \frac{K\lambda}{\beta cos\theta} \text{Å} \quad (2)$$

where D is the average crystallite size in Å, K is the shape factor (0.9), K is the wavelength of X-ray (1.5406 Å) Cu Kα radiation, θ is the Bragg angle, and β is the corrected line broadening of NPs [16]. The average crystallite size of ZnO NPs is about 11.9 nm.

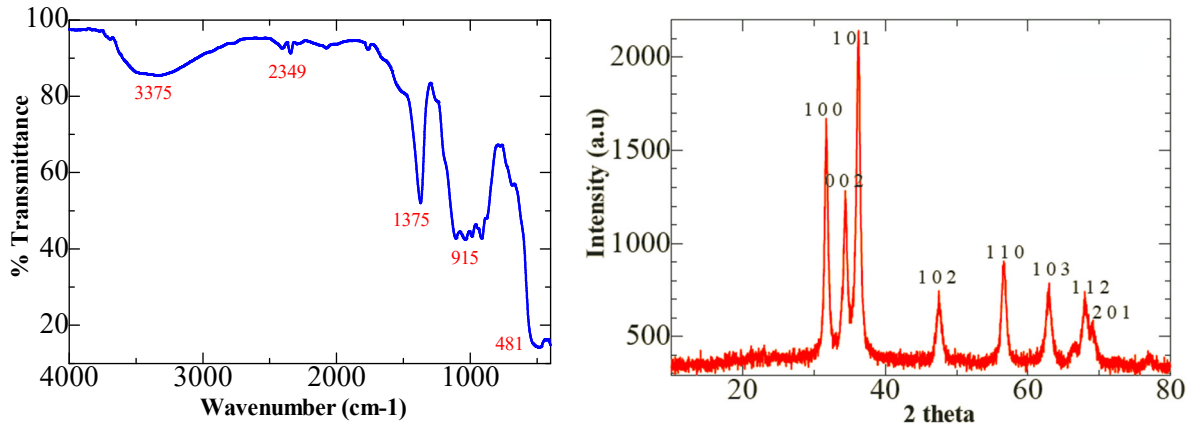

(a) (b)

Figure 3. (a) FT-IR spectra and (b) powder X-ray diffraction of biosynthesized ZnO NPs.

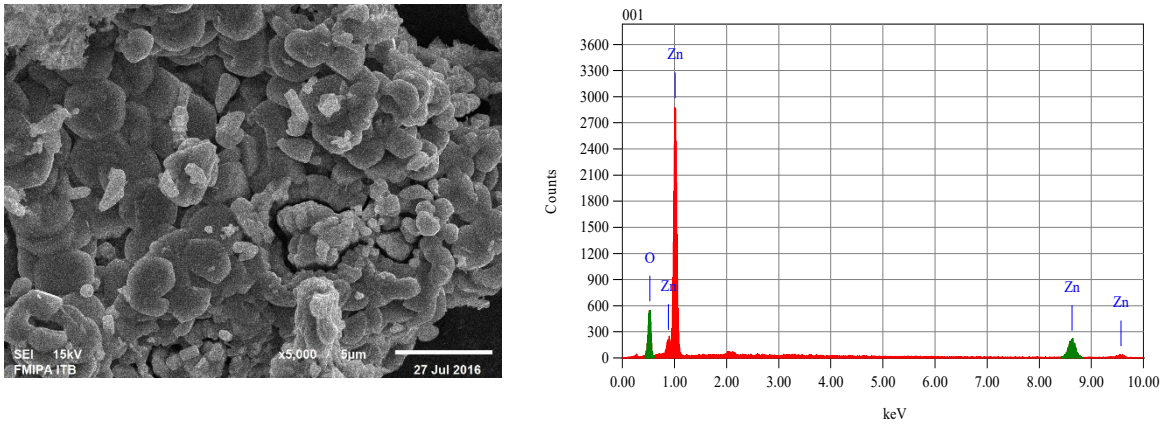

(a) (b)

Figure 4. Biosynthesized ZnO NPs (a) SEM image (b) EDS spectrum.

3.4. SEM-EDS analysis

The morphology of biosynthesized ZnO NPs was observed by SEM, as shown in figure 4a. The diameter of cluster ZnO NPs was 2 μm and in hexagonal nanochip shape with rough surface. The EDS analysis confirmed the chemical composition of ZnO NPs as shown in the figure 4b. The EDS spectrum shows the high value of zinc (80.3%) and oxygen (19.65%), respectively.

4. Conclusions

The ZnO NPs were successfully biosynthesized by sol-gel method using *Imperata cylindrica L.* leaf extract as base source and stabilizing agent. Hydrolysis process showed the characteristic absorption peak of $Zn(OH)_2$ at λ_{max} 300 nm and UV-Vis-DRS data confirmed the indirect band gap at 3.13 eV. FT-IR spectra revealed the functional groups of stretching bands of ZnO NPs around 600-400 cm^{-1}. The XRD result showed the sample was well crystallized in a hexagonal wurtzite structure with crystallite size of 11.9 nm. SEM-EDS analysis showed the morphology of hexagonal nanochip with the compositions of Zn and O elements.

Acknowledgements

The authors would like to thank Universitas Indonesia for funding this research through PITTA Grant Universitas Indonesia with contract No: 2039/UN2.R12/HKP.05.00/2016.

References

[1] Ariyanta H A and Yulizar Y 2016 *IOP Conf. Series: Materials Science and Engineering* **107** 012002-8
[2] Chen Y, Bagnall D M, Koh H, Park K, Hiraga K, Zhu Z and Yao T 1998 *J. Appl. Phys.* **84** 3912-8
[3] Ozgur U, Alivov Y I, Liu C, Teke A, Reschikov M A, Dogan S, Avrutin V, Cho S J and Morkoc H 2005 *J. Appl. Phys.* **98** 041301-103
[4] Darroudi M, Sabouri Z, Oskuee R K, Zake A K, Kargarc H and Hamid M H N A 2013 *Ceram. Int* **39** 9195-9
[5] Rathi Sre P R, Reka M, Poovazhagi R, Arul Kumar M and Murugesan K 2015 *Spectrochim. Acta A Mol Biomol Spectrosc.* **135** 1137-44
[6] Singh B N, Rawat A K S, Khan W, Naqvi A H and Singh B R 2014 *PloS ONE* **9 e**106937-12
[7] Yuvakkumar R, Suresh J, Nathanael A J, Sundrarajan M and Hong S I 2014 *Mat. Sci. Eng. C* **41** 17-27
[8] Raliya R *et al.* 2014 *Int. J. Biol. Macromol* **65** 362-8
[9] Elumalai K, Velmurungan S, Ravi S, Kathiravan V, Ashokkumar S 2015 *Molecular and Biomolecular Spectroscopy* **143** 158-64
[10] Zhong Y Z, Wang M H and Liu T T 2015 *Materials Letters* **158** 274-7
[11] Udawatte N, Lee M, Kim J and Lee D 2011 *ACS Appl. Mater. Interfaces* **3** 4531-8
[12] Habibi M H and Rahmati M H 2015 *Spectrochim.Acta A* **137** 160-4
[13] Fu L and Fu Z 2015 *Ceramics International* **41** 2492-6
[14] Diallo A, Ngom B D, Park E and Maaza M 2015 *Journal of Alloys and Compounds* **646** 425-30
[15] Thema F T, Manikandan E, Dhlamini M S and Maaza M 2015 *Materials Latters* **161** 124-7
[16] Ramesh M, Anbuvannan M and Viruthagiri G 2015 *Molecular and Biomolecular Spectroscopy* **136** 864-70
[17] Peletiri C, Matur B M, Ihongbe J C and Okoye M 2012 *J. Med. Sci.* **2(1)** 013-7
[18] John R and Rajakumari R 2012 *Nano-Micro Lett.* **4(2)** 65-72